Inorg. Chem. **2003**, *42*, 8682–8689

Structural Study on Highly Oxidized States of a Water Oxidation Complex $[Ru^{III}(bpy)_2(H_2O)]_2(\mu\text{-}O)^{4+}$ by Ruthenium K-Edge X-ray Absorption Fine Structure Spectroscopy

Kaoru Okamoto,[†] Jun Miyawaki,[†] Kensuke Nagai,[†] Daiju Matsumura,[†] Akihiro Nojima,[†] Toshihiko Yokoyama,[‡] Hiroshi Kondoh,[†] and Toshiaki Ohta*[,†]

Department of Chemistry, School of Science, The University of Tokyo, Tokyo 113-0033, Japan, and Institute for Molecular Science, Okazaki 444-8585, Japan

Received April 7, 2003

The oxidation-induced structural change of a water-oxidizing diruthenium complex, $[(bpy)_2(H_2O)Ru^{III}(\mu\text{-}O)Ru^{III}(OH_2)(bpy)_2]^{4+}$ (bpy = 2,2′-bipyridine), was investigated by means of X-ray absorption spectroscopy. Ru K-edge XANES (X-ray absorption near-edge structure) spectra from the acidic solution and solid precipitates obtained by oxidation showed that the absorption edge shifts toward higher energy with a preedge feature slightly more enhanced than those of the lower oxidation states. This indicates that the higher oxidation state has a lower symmetry due to shortening of the Ru–O bonds that originated from the water ligands. The EXAFS (extended X-ray absorption fine structure) spectra were similar to those of the lower oxidation states, whose analysis revealed the existence of short Ru–O double bonds and an almost linear Ru–O–Ru angle (169 ± 2°). Ab initio EXAFS simulations for several possible structural models suggest that the dimeric structure is maintained during the water oxidation reaction.

Introduction

Photosynthesis by oxygen-evolving organisms is achieved by two functional parts. Water molecules are converted to dioxygen by photochemical oxidation in photosystem II, while the resulting four electrons are transferred to photosystem I to be used in the production of sugars from carbon dioxide. Since the photosystem II is very attractive as a highly efficient and clean oxygen/electron source, the reaction detail has been extensively studied from an energetic aspect. The reaction center contains an oxygen-bridged Mn_4 cluster, which is oxidized stepwise by photoinduced electron elimination until four electrons are taken off before water oxidation.[1] Although the phenomenon is well-known, the crystal structure of the reaction center has been analyzed very recently,[2] and the reaction process has not been fully understood yet. A number of functional or structural model compounds have been synthesized to mimic the photosystem II.[3] The net reaction in photosystem II is as follows:

$$2H_2O \rightarrow O_2 + 4H^+ + 4e^-$$

Because it is a thermodynamically and mechanistically demanding reaction, the water oxidation has not been achieved in many single-molecular systems that have a reaction center similar to photosystem II. An oxygen-bridged diruthenium complex, $[(bpy)_2(H_2O)Ru^{III}(\mu\text{-}O)Ru^{III}(OH_2)(bpy)_2]^{4+}$ (bpy = 2,2′-bipyridine), is one of the promising model systems. It produces dioxygen from water catalytically as a consequence of stepwise four-electron chemical or electrochemical oxidation in aqueous solutions and has been studied in detail using UV−vis, Raman, electron paramagnetic resonance (EPR), and cyclic voltammetry techniques from the static and kinetic aspects.[4] The complex oxidation is coupled with some proton loss at each step, which stabilizes the Ru centers to achieve a highly oxidized reaction center. The basic structure of the complex seems to be maintained during the water-oxidation reaction, and the

* To whom correspondence should be addressed. E-mail: ohta@chem.s.u-tokyo.ac.jp. Tel: +81-3-5841-4333. Fax: +81-3-3812-1896.
† The University of Tokyo.
‡ Institute for Molecular Science. Tel: +81-564-55-7345. Fax: +81-564-55-4639.

(1) (a) Debus, R. J. *Biochim. Biophys. Acta* **1992**, *1102*, 269. (b) Kok, B.; Forbush, B.; McGloin, M. *Photochem. Photobiol.* **1970**, *11*, 457.
(2) Zouni, A.; Witt, H.-T.; Kern, J.; Fromme, P.; Krauss, N.; Saenger, W.; Orth, P. *Nature* **2001**, *409*, 739.
(3) (a) Manchanda, R.; Brudvig, G. W.; Crabtree, R. H.; *Coord. Chem. Rev.* **1995**, *144*, 1. (b) Rüttinger, W., Dismukes, G. C. *Chem. Rev.* **1997**, *97*, 1.

10.1021/ic034373n CCC: $25.00
Published on Web 12/02/2003

oxygen-bridged dimer structure would be one of the keys for the reaction. However, the oxygen-evolving mechanism is still an open question, partly because the oxidation process is very complicated, including complex anion substitution and cross electron transfer reactions, and partly because only little information has been obtained for its highly oxidized states. The reactive species revealed to be the four-electron-oxidized complex, [5,5],[5] at least in acidic media, while it may be in the lower oxidation states under neutral conditions[4k] or for the 4,4′- and 5,5′-dicarboxy-2,2′-bipyridine derivatives,[4c] and the intermediate oxidation states are still under hot discussion. The X-ray structure is known only at low oxidation states: the starting [3,3] state[4b] and the one-electron-oxidized state, [3,4].[4f] Raman spectroscopic studies indicated that the water ligands are deprotonated in the high oxidation states to give Ru═O double bonds and that the Ru−O−Ru bonding stays nearly linear,[4d] but no direct evidence for their structure has been obtained. Especially the latter is one of the critical points that determine the reaction mechanism; if the oxygen evolution occurs within one molecule, the Ru−O−Ru bridge must be bent to enable the O−O interaction, while it does not have to be in the intermolecular reactions.

X-ray absorption fine structure (XAFS) spectroscopy is one of the powerful tools for the electronic and structural studies. X-ray absorption near-edge structure (XANES) reflects the electronic state and coordination environment of the X-ray absorbing atom, while extended X-ray absorption fine structure (EXAFS) shows the local structure around the absorbing atom. Since it does not require long-range ordering, it is applicable to surfaces, particles, liquids, and solutions, irrespective of the sample form. The purpose of this study is to elucidate the local structure around the Ru atoms in acidic media, especially the Ru−O−Ru angle, using XAFS spectroscopy.

Experimental Section

Sample Preparations. $[Ru^{III}(bpy)_2(H_2O)]_2(\mu\text{-}O)(ClO_4)_4\cdot 2H_2O$ (denoted as [3,3][5]) was synthesized according to the literature.[4b] It was purified for several times monitoring the UV−vis spectra. Solid $[Ru^{III}(bpy)_2(H_2O)][Ru^{IV}(bpy)_2(OH)](\mu\text{-}O)(ClO_4)_4\cdot 2H_2O$ ([3,4]) was prepared by adding ∼1 equiv of solid $Ce^{IV}(NH_4)_2(NO_3)_6\cdot 4H_2O$ before the addition of a saturated aqueous solution of $NaClO_4$ in the recrystallization process.[4f] Higher oxidation states were achieved by adding an equivalent or excess amount (ca. 3−20 equiv) of $Ce^{IV}(NH_4)_2(NO_3)_6\cdot 4H_2O$ to acidic solutions of [3,4] freshly prepared from [3,3]. *Warning: perchlorate salts are potentially explosive! Great care should be paid in storing and handling.* All other chemicals were used as received.

XAFS Measurements. Ru K-edge XAFS experiments were carried out at BL-10B at the Photon Factory of the Institute of Materials Structure Science (KEK-PF; typical operation energy of 2.5 GeV and stored current of 450−300 mA),[6] using a channel-cut Si(311) monochromator, and at BL01B1 at SPring-8 of the Japan Synchrotron Radiation Research Institute (operation energy of 8 GeV and stored current of 70−50 mA),[7] using a double-crystal Si(311) monochromator and Rh-coated mirrors. The incident and transmitted X-rays were detected by ion chambers filled with 50% Ar−50% N_2 and pure Ar, respectively, and the fluorescent X-rays by a Lytle detector filled with Xe. Although the absolute photon energy was not calibrated, the relative photon energy calibration was performed using the inflection point of the absorption edge for solid [3,3] with the accuracy of 0.9 eV.

Solid [3,3] and [3,4] were diluted with BN powder (∼30%) to be pressed into pellets (6.5 mm diameter, ∼1 mm thickness) and cooled to ∼30 K using a closed-cycle He cryostat monitored with a Si diode thermometer. Solution sample (typically ∼0.010 M) in 1 M aqueous trifluoromethanesulfonic acid was introduced to a polypropylene bag with a Teflon spacer (10 or 20 mm thickness) and measured at room temperature. Since the higher oxidation states easily oxidize organic materials, polyethylene bags cannot be used as shown by a fast reduction of a [3,4] solution to [3,3]. Polypropylene seems to be stable at least for the measurement period enough to allow the water-oxidation reaction. These solid and solution samples were measured in the transmission mode.

For oxidation states higher than that of [3,4], samples were also prepared in two other ways. One was a solution, which was quickly transferred to a Pyrex cell (10 mm diameter, 5 mm thickness) after adding 4 equiv of Ce^{4+} in total and mixing and then cooled by liquid N_2 and sealed in a vacuum. Another was a precipitated solid produced by adding an excess amount (∼10 equiv) of Ce^{4+}, followed by quick filtering with a glass filter and immediate cooling. They both were cooled by a cryostat and measured in the fluorescence X-ray yield mode, because the samples were not always homogeneous in these cases. Each preparation method gave the same spectra without time dependence for several measurements.

Data acquisition times were 1 and 16 s per point for the XANES and EXAFS measurements at the longest, respectively.

Results

Figure 1 shows the Ru K-edge XANES spectra of [3,3], [3,4], and the higher oxidation state samples. Solid and solution samples in each state gave the same spectra. They all showed the typical shape of Ru O_h complex[8] with a small edge shift to a higher energy at each oxidation step. This suggests that the coordination environment around the Ru

(4) (a) Gersten, S. W.; Samuels, G. J.; Meyer, T. J. *J. Am. Chem. Soc.* **1982**, *104*, 4029. (b) Gilbert, J. A.; Eggleston, D. S.; Murphy, W. R.; Geselowitz, D. A.; Gersten, S. W.; Hodgeson, D. J.; Meyer, T. J. *J. Am. Chem. Soc.* **1985**, *107*, 3855. (c) Rotzinger, F. P.; Munavalli, S.; Comte, P.; Hurst, J. K.; Gratzel, M.; Pern, F.-J.; Frank, A. J. *J. Am. Chem. Soc.* **1987**, *109*, 6619. (d) Hurst, J. K.; Zhou, J.; Lei, Y. *Inorg. Chem.* **1992**, *31*, 1010. (e) Hurst, J. K.; Lei, Y. *Inorg. Chem.* **1994**, *33*, 4460. (f) Schoonover, J. R.; Ni, J. F.; Roecker, L.; White, P. S.; Meyer, T. J. *Inorg. Chem.* **1996**, *35*, 5885. (g) Chronister, C. W.; Binstead, R. A.; Ni, J.; Meyer, T. J. *Inorg. Chem.* **1997**, *36*, 3814. (h) Binstead, R. A.; Chronister, C. W.; Ni, J.; Hartshorn, C. M.; Meyer, T. J. *J. Am. Chem. Soc.* **2000**, *122*, 8464. (i) Lebeau, E. L.; Ajao Adeyemi, S.; Meyer, T. J. *Inorg. Chem.* **1998**, *37*, 6476. (j) Yamada, H.; Hurst, J. K. *J. Am. Chem. Soc.* **2000**, *122*, 5303. (k) Raven, S. J.; Meyer, T. J. *Inorg. Chem.* **1988**, *27*, 4478. (l) Comte, P.; Nazeeruddin, M. K.; Rotzinger, F. P.; Frank, A. J.; Grätzel, M. *J. Mol. Catal.* **1989**, *52*, 63.

(5) Hereafter the oxidation states are designated using the formal electronic states of the ruthenium ions as [3,3] for $[(bpy)_2(H_2O)Ru^{III}(\mu\text{-}O)Ru^{III}(OH_2)(bpy)_2]^{4+}$. Note that the hydrogen number may be changed in the same designation and that there should be strong electronic interactions between two Ru centers through the oxygen bridge and the assignment of the oxidation states is equivocal.

(6) Nomura, M.; Koyama, A. *KEK Rep.* **1989**, *89*, 16.

(7) Uruga, T.; Tanida, H.; Yoneda, Y.; Takeshita, K.; Emura, S.; Takahashi, M.; Harada, M.; Nishihata, Y.; Kubozono, Y.; Tanaka, T.; Yamamoto, T.; Maeda, H.; Kamishima, O.; Takabayashi, Y.; Nakata. Y.; Kimura, H.; Goto, S.; Ishikawa, T. *J. Synchrotron Radiat.* **1999**, *6*, 143.

(8) Okamoto, K.; Takahashi, T.; Kohdate, K.; Kondoh, H.; Yokoyama, T.; Ohta, T. *J. Synchrotron Radiat.* **2001**, *8*, 689.

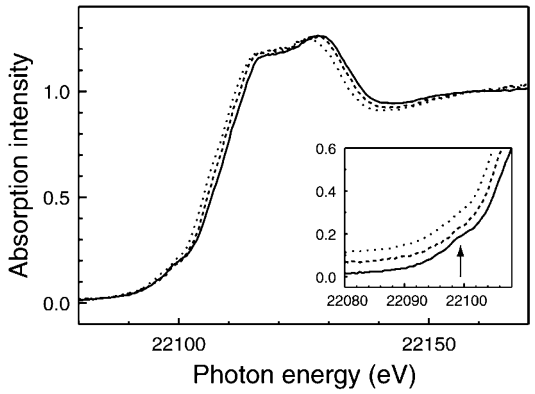

Figure 1. Ru K-edge XANES spectra for [3,3] (dotted line), [3,4] (dashed line), and a highly oxidized state (solid line). Inset: Enlargement of the preedge features at ~22 100 eV, in which the spectra are shifted vertically for clarity.

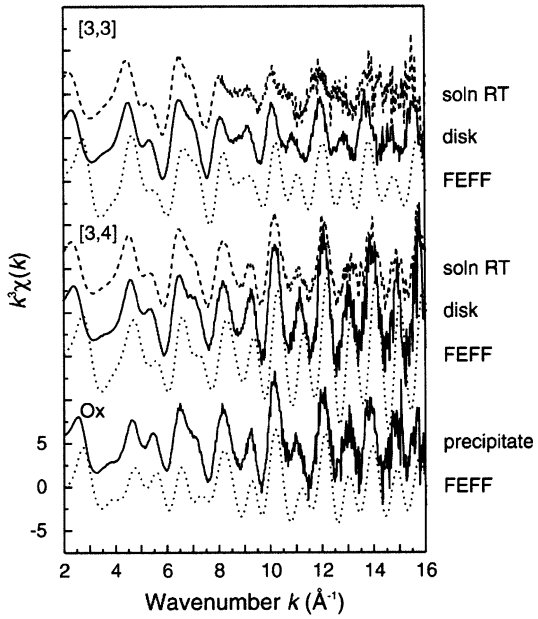

Figure 2. Ru K-edge EXAFS $k^3\chi(k)$ spectra at various oxidation states, [3,3], [3,4], and the higher oxidation state (Ox) measured using solution and solid samples (dashed and solid lines, respectively), and simulated by FEFF8.10 (dotted lines).

ion is maintained during the oxidation process. The inset in Figure 1 is an expansion of the preedge region. One can see a slight enhancement of a shoulder at 22 098 eV in the highly oxidized sample, which may be assigned to the 1s → 4d transition as is for a molybdenum−nitrogen complex.[9] It is formally dipole-forbidden and weakly quadrupole-allowed in centrosymmetric systems but gains some intensity in a lower symmetry by mixing with p orbitals. The enhancement of this feature supports slight symmetry lowering, which might be related to a shortened bond between the ruthenium and oxygen from the water ligand (hereafter denoted as O_w) as indicated from the Raman spectroscopic study.[4d]

EXAFS $k^3\chi(k)$ spectra and corresponding Fourier transforms ($\Delta k_{FT} \sim 4-15.5$ Å^{-1}) are shown in Figures 2 and 3, respectively, for solution samples at room temperature and

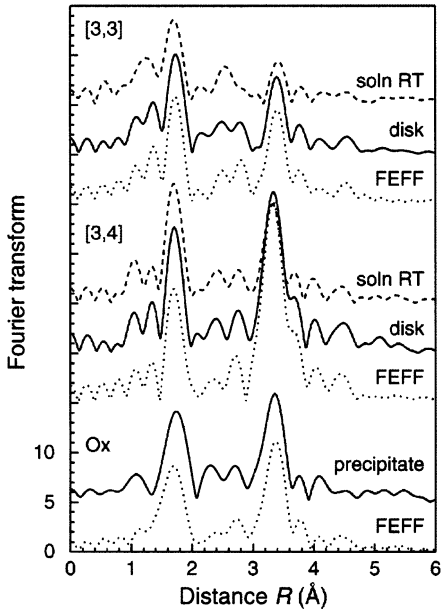

Figure 3. Ru K-edge EXAFS Fourier transforms at the [3,3], [3,4], and higher (Ox) oxidation states measured using solution and solid samples (dashed and solid lines, respectively) and simulated with FEFF8.10 (dotted lines).

for solid samples at 30 K. The EXAFS oscillation function was obtained by standard procedures: preedge baseline subtraction; postedge background estimation using a cubic spline function; normalization with the atomic absorption coefficient given in the literature.[10,11] They all look alike as the XANES spectra do, again indicating similar dimeric structures. Figure 4 also shows the EXAFS spectra of the highly oxidized solution and solid samples for the shorter k range. Although the data above $k \sim 12$ Å^{-1} were not used because of a low S/N ratio for the solution, they are similar to each other, indicating that the two samples were in the same state. The 1−2 Å peaks in the Fourier transforms are attributed to the Ru−O,N scattering in the first coordination shells, the 2−3 Å ones to the Ru−C2,6 single scattering and Ru−N−C2,6 double scattering in the bpy ligands, and the 3−4 Å ones to the bridging Ru−O−Ru and ligand Ru−C3,5 single and multiple scattering (see Figure 5).

For [3,3] and [3,4], EXAFS spectra were simulated by the ab initio program FEFF8.10[12] for the known X-ray structures,[4b,f] which gave good agreement with the experimental spectra as shown in Figures 2 and 3. It should be noted that the Fourier transform feature around 1 Å is weakened in the simulated spectrum for the higher oxidation state (see below for the simulation details). It is due to the fact that the Ru−O_w bond shortening by proton loss causes the interference among Ru−O_w, Ru−(μ−O), and Ru−N scatterings. Thus, the intensity reduction in this region observed in the experimental spectrum would suggest the Ru−O_w bond shortening in the higher oxidation state.

(9) Laplaza, C. E.; Johnson, J. A.; Peters, J. C.; Odom, A. L.; Kim, E.; Cummins, C. C.; George, G. N.; Pickering, I. J. *J. Am. Chem. Soc.* **1996**, *118*, 8623.

(10) For instance: *X-ray Absorption: Principles, Applications, Techniques of EXAFS, SEXAFS and XANES*; Koningsberger, D. C., Prins, R., Eds.; Wiley: New York, 1988.

(11) Yokoyama, T.; Hamamatsu, H.; Ohta, T. *Computer code EXAFSH, Version 2.1*; The University of Tokyo: Tokyo, 1993.

(12) Ankudinov, A. L.; Ravel, B.; Rehr, J. J.; Conradson, S. D. *Phys. Rev. B* **1998**, *58*, 7565.

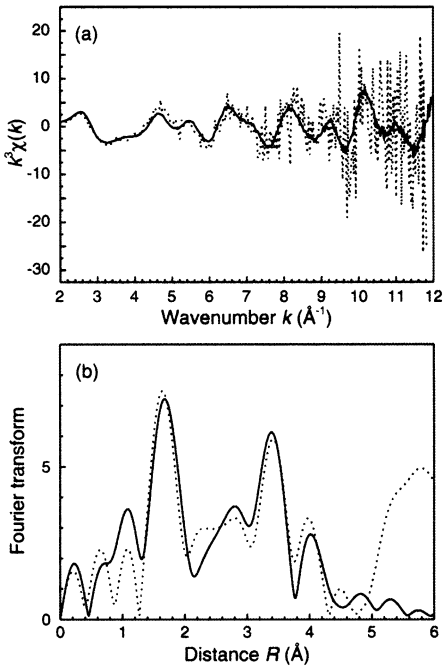

Figure 4. Ru K-edge EXAFS (a) $k^3\chi(k)$ spectra and (b) corresponding Fourier transforms for a short k range (4.2−11.8 Å^{-1}) of the highly oxidized solid (solid lines) and solution (dotted lines) samples.

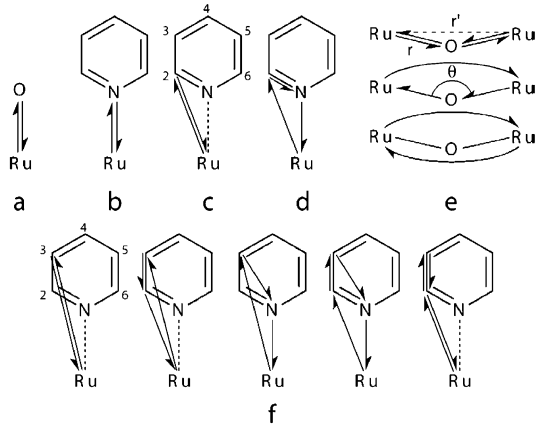

Figure 5. Selected paths for the curve-fitting analysis.

The 3−4 Å peak shifts to a shorter distance and has greater intensity in [3,4] and the highly oxidized states compared to that in [3,3]. Since the bpy coordination would cause little structural change upon oxidation, the difference should be attributed to the change in the Ru−O−Ru bridging structure. The Ru−O−Ru angles in [3,3] and [3,4] are 165.4[4b] and 170.0°,[4f] respectively. When three atoms are placed in a linear arrangement, the multiple scattering among them becomes more significant compared with a bent structure. It is called the focusing or shadowing effect,[10] which is quite sensitive to the bond angle. The increase of the 3−4 Å peak from [3,3] to [3,4] is explained as an enhanced focusing in a more linear Ru−O−Ru bridge of [3,4]. The highly oxidized precipitate is also considered to have a relatively linear Ru−O−Ru bridging, and it is consistent with the previous DFT calculations.[13]

EXAFS curve-fitting analysis was performed for solid samples using the EXAFSH code[11] in the back Fourier transformed k-space with the fitting k range of ca. 4.5−15 Å^{-1}. Selected paths used in the fitting were depicted in Figure 5. Preliminarily, the first coordination shells ($\Delta R_{BFT} \sim 0.9-2$ Å) and the Ru−O−Ru and Ru−C3,5 shells ($\Delta R_{BFT} \sim 3-4$ Å) were separately fitted to determine the energy shifts ΔE_0, and then all paths within the ΔR_{BFT} range of 0.9−4 Å were fitted with interatomic distances R and Debye−Waller factors C_2 as variables. The higher order cumulants of the Debye−Waller factor were neglected. The intrinsic loss factors s_0^2 were set to the best-fit values of 0.95 and 1.0 for [3,3] and [3,4], respectively, and the average value, 0.98, was set for the highly oxidized sample. The coordination numbers N were fixed to those of the proposed structures. Data refinement and error estimation were done according to the International XAFS Society report.[14] The backscattering amplitude and phase shift standards for each shell were derived from the calculated spectrum by FEFF8.10 on the basis of the X-ray structures of [3,3][4b] and [3,4].[4f] The spectrum of the higher oxidation state was fitted using the same standards as [3,4].

There are six atoms in the first coordination sphere of Ru: one O in the bridge (ca. 1.85 Å in the XRD results), one O from the ligated water (2.14 Å for H_2O and 1.98 Å for OH), and four N in the bpy ligands (2.07 Å in average). Because the radial resolution of EXAFS is estimated as $\pi/2\Delta k_{fit} \sim 0.13$ Å, the oxygen atom of water cannot be distinguished from the bpy nitrogen atoms. On the other hand, its distance from a highly oxidized Ru ion would be shorter by deprotonation to 1.72−1.74 Å,[13,15a] which seems difficult to distinguish from the bridging oxygen. Thus, these close shells were treated as one shell and the distance deviations were included into the static components of C_2. The 3−4 Å shells were analyzed as the single, double, and triple scattering of Ru−O−Ru and Ru−C3,5 (paths e and f in Figure 5, respectively).

The curve-fitting results with the fitting R-range of 0.9−4 Å are summarized in Table 1, and the back Fourier transformed experimental and fitted $k^3\chi(k)$ curves are shown in Figure 6. The filtered analyses for 0.9−2 Å and 3−4 Å gave the same R and C_2. The interatomic distances obtained from the X-ray diffraction study of [3,3][4b]/[3,4][4f] are 1.869/1.835 Å for the bridging O, 2.072/2.078 Å for N's in bpy and O's in water ligands, and 3.724/3.663 Å for Ru−O−Ru (averages for three paths in Figure 5e). The fitting results are well consistent with these values. The better fit was obtained for the first peak of the highly oxidized sample when O_w was included in the bridging O shell rather than in the N shell, though the relatively large C_2 value for oxygen

(13) Bartolotti, L. J.; Pedersen, L. G.; Meyer, T. J. *Int. J. Quantum Chem.* **2001**, *83*, 143.

(14) The International XAFS Society Committee, http://ixs.csrri.iit.edu/subcommittee_reports/sc/err-rep.pdf, 2000.

(15) (a) Dengel, A. C.; El-Hendawy, A. M.; Griffith, W. P.; O'Mahoney, C. A.; Williams, D. J. *J. Chem. Soc., Dalton Trans.* **1990**, 737. (b) Neubold, P.; Della Vedova, B. S. P. C.; Wieghardt, K.; Nuber, B.; Weiss, J. *Inorg. Chem.* **1990**, *29*, 3355. (c) Bardwell, D.; Jeffery, J. C.; Joulié, L.; Ward, M. D. *J. Chem. Soc., Dalton Trans.* **1993**, 2255. (d) Bardwell, D.; Horsburgh, L.; Jeffery, J. C.; Joulié, L. F.; Ward, M. D.; Webster, I.; Yellowless, L. J. *J. Chem. Soc., Dalton Trans.* **1996**, 2527.

Table 1. Curve-Fitting Results with Values in Parentheses Being Estimated Errors for the Last Digit

	$Ru^{III}ORu^{III}$		$Ru^{III}ORu^{IV}$		oxidized state	
	R (Å)	10^2C_2 (Å^2)	R (Å)	10^2C_2 (Å^2)	R (Å)	10^2C_2 (Å^2)
1 Ru−(μ-O)	1.87(2)	0.1(2)	1.84(1)	0.0(1)		
5 Ru−N/O_w	2.07(1)	0.3(1)	2.07(1)	0.3(1)		
2 Ru−(μ-O)/O_w					1.82(4)	0.8(5)
4 Ru−N					2.08(1)	0.3(1)
8 Ru−C2/C6	3.00(4)	0.9(4)	3.00(3)	0.8(2)	2.98(3)	0.7(3)
1 Ru−O−Ru	3.74(2)	0.3(1)	3.689(6)	0.13(5)	3.70(1)	0.23(8)
8 Ru−C3/C5	4.42(8)	1(1)	4.40(7)	1(1)	4.4(1)	1(1)
ΔE_0 (eV)	−5.5	−3.5	−5.5			
R-factor[a] (%)	14.9	8.91	14.9			
f[b]	5.5	3.0	3.5			
$(\Delta\chi)^2$[b]	1.09	1.06	1.17			
∠(Ru−O−Ru)[c] (deg)	165(1)	170(2)	169(2)			

[a] $R\text{-factor} = 100 \times \{[\sum_i |k_i^3\chi_{iobs}(k_i) - k^3\chi_{icalc}(k_i)|^2]/[\sum_i |k_i^3\chi_{iobs}(k_i)|^2]\}^{1/2}$%. [b] $(\Delta\chi)^2 = \{N_{ind}/[N(N_{ind} - N_p)]\}\sum_{i=1}\{[N|k_i^3\chi_{iobs}(k_i) - k^3\chi_{icalc}(k_i)|^2]/(f\epsilon)^2\}$, where N is the number of data, N_p the number of parameters, and ϵ the error estimated from the rms amplitude of the R-space Fourier transform between 15 and 25 Å with the scaling factor f that was determined to give $(\Delta\chi)^2$ of ca. 1.[14] [c] Errors are estimated from those of the coordination numbers (∼0.1).

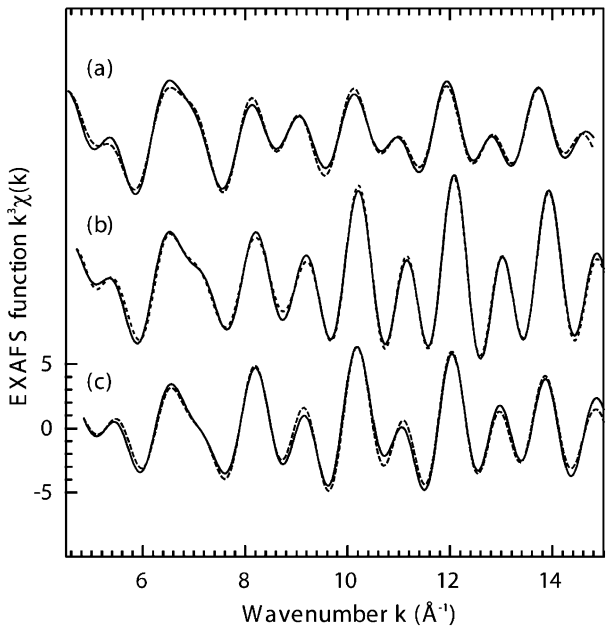

Figure 6. Back Fourier transformed experimental (solid lines) and fitted (dashed lines) $k^3\chi(k)$ of (a) [3,3], (b) [3,4], and (c) highly oxidized states.

atoms indicates that the difference between the distances are not very small. Three-shell analysis in this region was also performed and gave the distances of one 1.77- and one 1.95-Å oxygen atoms and four 2.07-Å nitrogen atoms. As the obtained Ru−O−Ru distance is 3.70 Å, the 1.77- and 1.95-Å bonds should be the Ru−O_w and Ru−(μ-O) bonds, respectively. However, the long Ru−(μ-O) bond gives the Ru−O−Ru angle θ of ∼140°, which contradicts a nearly linear Ru−O−Ru bridge structure as discussed above. Since the focusing effect diminishes rapidly as the angle θ decreases, such intense scattering does not occur for the structure with θ of 140°. Thus, we conclude that the three-shell fitting gives unreasonable results for the present case.

To evaluate the Ru−(μ-O) distance and the Ru−O−Ru angle θ in the highly oxidized state, we used the following procedure. Since the peaks at 3−4 Å are mainly associated with the Ru−O−Ru scattering, they were filtered in the r-space and Fourier transformed back to the k-space. The curve fitting analysis was performed at a fixed Ru−O−Ru angle (θ = 150−180° with 1° step) to optimize N, R, and C_2. It is known that the focusing effect is mainly on the backscattering amplitude.[10] In the analysis, the backscattering amplitude and phase shift were extracted from the FEFF calculations for the Ru−O−Ru three-atom system at each angle. Figure 7 shows R-factors and coordination numbers N plotted as a function of the angle θ. R-factors are rather insensitive to θ, but N's show large dispersion with θ. Since N is known to be 1.0 in every case, we determined the angle at which N is equal to 1. The angles obtained are 165 ± 1° and 170 ± 2° for [3,3] and [3,4] solids, respectively, which are both in good agreement with the X-ray crystal structures,[4b,f] and 169 ± 2° for the oxidized precipitate. It should be noted that the Debye−Waller factors C_2 were almost constant irrespective of θ. In the DFT calculations θ becomes larger upon oxidation up to 178° in the [5,5] state.[13] The present EXAFS result supports that θ at the highly oxidized state is almost linear, though it indicates that θ is as large as, or slightly smaller than, that of [3,4].

The Ru−O−Ru angle θ is correlated with the Ru−(μ-O) and Ru−Ru distances r and r', respectively, by the following equation: $\sin(\theta/2) = r'/2r$. The distance obtained from the curve-fitting analysis is the average of the three paths in Figure 5e, $R_{av} = (r' + 2r)/2$. From these relationships, the calculated r and r' from θ and R_{av} are 1.85 and 3.69 Å, respectively. Since the average of Ru−(μ-O) and Ru−O_w distances is 1.82 Å as obtained by the curve-fitting analysis (Table 1), the latter should be 1.79 Å. Although this is longer than those of the analogous complex[15a] and of the DFT calculations,[13] it is much shorter than the H_2O and OH ligands, indicating a double-bonded oxo ligand. FEFF calculations using these Ru−O distances also give sufficiently good agreement with the experimental data as shown in Figures 2 and 3.

Discussion

XAFS Measurements. Sample homogeneity is strictly required in the transmission X-ray detection method as is in other transmission spectroscopies. In the present experiments, the oxygen-evolving species produces gaseous O_2 from H_2O within minutes by addition of the oxidant. The relatively fast reaction and accompanying gas bubbles made in-situ XAFS measurements difficult at room temperature. The in-situ

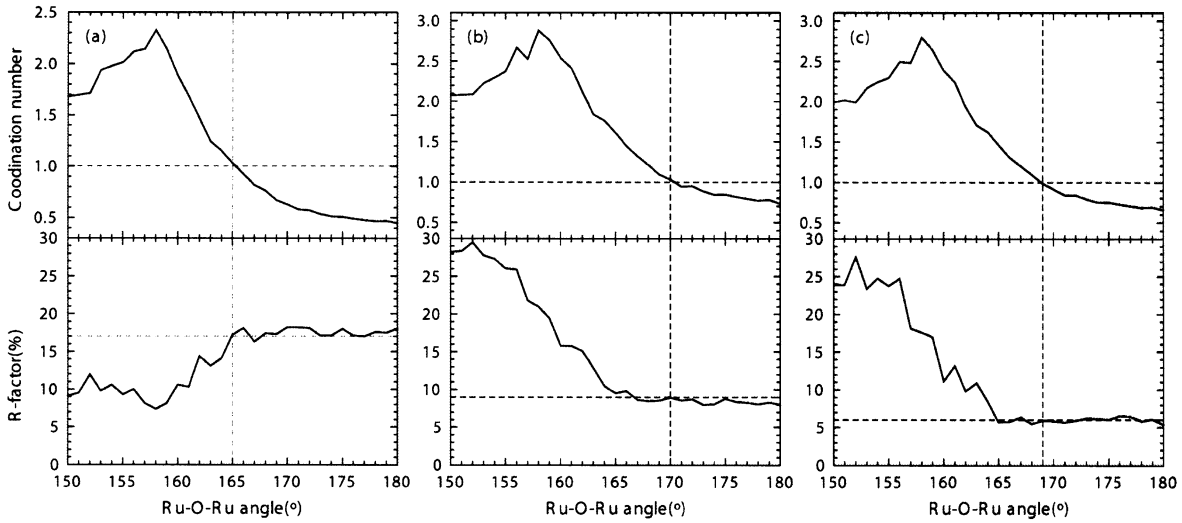

Figure 7. Results of the Ru−O−Ru angle determination for (a) [3,3], (b) [3,4], and (c) highly oxidized states. Upper and lower figures plot the coordination number and *R*-factor (%) as a function of the Ru−O−Ru angle, respectively. The angle is determined to be what gives the accurate coordination number.

XANES spectra show a slight enhancement of the preedge feature compared with [3,4], but large noises and breaks due to quick scanning and gas bubbles prevented more detailed discussion. They were much more serious in the EXAFS spectra since the EXAFS oscillations are very weak. The reaction becomes slower to some extent by cooling the solution to ca. −5 °C, as estimated from the time dependence of the UV−vis absorbance. However, in this case the solubility of the oxidized sample becomes lower to give large amount of precipitate from a nearly saturated sample solution prepared for the transmission XAFS measurement. By these reasons, the fluorescent X-ray yield method was adopted at a low temperature. It usually requires less sample homogeneity and thus is applicable for the frozen solutions or roughly mounted solid samples, while the signal intensity is very small due to large transmissivity of the high-energy X-rays as the Ru K-edge. The small signal might partly be related to much lower S/N ratio for the frozen solution sample in a Pyrex cell, which absorbs more fluorescent X-rays than a polypropylene bag used for the precipitate does.

Precipitation from the highly oxidized solutions was mentioned in some previous reports.[4] It happens under high concentrations of the dimer and/or the oxidant in perchlorate-containing solutions rather than trifluoromethanesulfonate solution, and the precipitate redissolved after 1 or 2 h with dioxygen evolution giving a [3,4] solution. Binstead et al. reported that the resonance Raman spectrum of the suspension had two peaks at 816 and ∼357 cm^{-1} attributable to ν_s(Ru−O−Ru) and ν(Ru═O), respectively, and a broad band at around 650 cm^{-1}.[4h] The first two features suggested that the precipitate is in the [5,5] state. Precipitation would be the result of the oxidation coupled with proton loss from the ligated water, while other possible origins, such as anion substitution, dimerization of dimers,[4h] and interaction with Ce^{4+},[4j] were also proposed.

In this work, the precipitate appeared with only small excess of oxidant even in trifluoromethanesulfonic acid, and the amount became larger at lower temperatures. It gave essentially the same XANES and EXAFS spectra with the solution, although the latter has too low S/N ratios to perform a quantitative analysis (Figure 4), and the frozen solution restarted the oxygen-evolving reaction when warmed to the room temperature several hours after adding the oxidant. These facts indicate that the precipitate should be the same species as that in the solution, which has smaller solubility in water than the lower oxidation state species possibly due to the deprotonation from the water ligands. The high reproducibility in several runs, together with the same XANES shapes with a small shift (vide infra), suggests that the contents of the lower oxidation state species such as [3,4] were negligible.

Electronic State of the Highly Oxidized Complex. Much has been discussed concerning the oxidation states higher than the one-electron oxidation state, [3,4]. The four-electron oxidation product [5,5] is regarded as the active species according to the electrochemical and spectroscopic studies,[4] although the existence of a short-lived higher oxidation state cannot be excluded. The [5,5] state is long believed to be the product of one-step three-electron oxidation of [3,4] at pH 0 and of one-electron oxidation of the intermediate [4,5] state in less acidic media, while Yamada et al. recently reported that the intermediate state is [4,4] by Os(bpy)$_3^{3+}$ oxidative titration, which can exist even in strongly acidic media.[4j] Although it is contradictory to the previous electrochemical studies, the latter assignment is consistent with the resonance Raman spectrum of the intermediate; there was no band attributable to ν(Ru═O), which should appear in Ru^{V}-containing states. The accumulating species are still undecided between the [4,5] and [5,5] states, which were detected as the ∼500 nm band in the UV−vis spectra for about 10 min. For the 4,4′- and 5,5′-substituted complexes, the [4,4] states do exist as two-electron oxidants toward water oxidation.[4c,l]

The XANES spectra are related to the electronic state and the coordination environment of the X-ray absorbing atom. The absorption edge position often shifts to higher energy

Chart 1

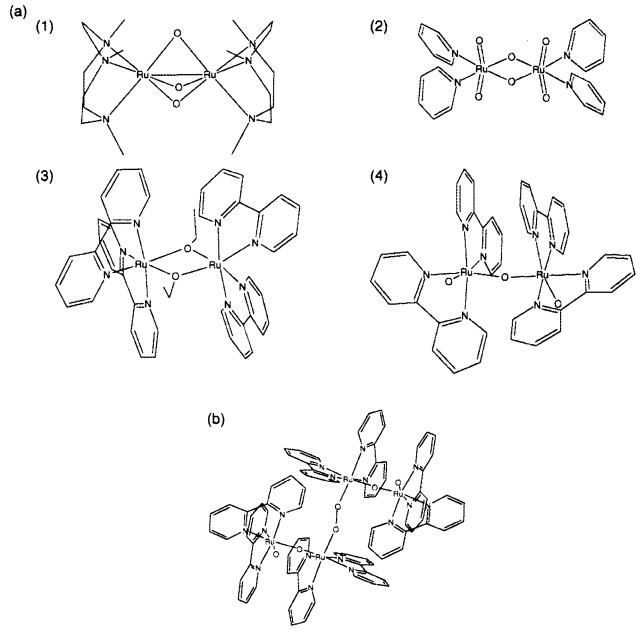

when the absorbing atom is oxidized without the coordination symmetry change. In fact, the XANES spectra in Figure 1 show that the highly oxidized sample has the absorption edge surely at a higher energy than the other two with similar coordination environments. However, the present system is very complicated due to the heavy element (Ru) absorption and it is difficult to estimate the oxidation state only from a small edge shift.

Another significant feature in the XANES spectra is the preedge peak. The [3,4] state with one Ru−OH and one Ru−OH_2 bonds shows a very small enhancement of this peak compared with that in the [3,3] state with two Ru−OH_2 bonds. Further enhancement from [3,4] to the higher oxidation state indicates the existence of short Ru═O bonds, which is consistent with the EXAFS curve-fitting result. Since the present experiments were performed in strongly acidic solutions, the oxo ligands bonding to Ru^{IV} should be protonated. These facts strongly suggest that the observed sample was in the [5,5] state.

Possible Structures of the Highly Oxidized Complex. As described above, previous studies mentioned the possibility of further dimerization. Binstead et al. attributed the Raman band at ∼650 cm^{-1} to a "dimer-of-dimers" structure with a diamond core, [(O)$(bpy)_2$RuORu$(bpy)_2$(μ-$O)_2$$(bpy)_2$RuORu$(bpy)_2$(O)], on the analogy of an Fe_2(μ-$O)_2$ complex with a Raman band at 667 cm^{-1}.[4h,16] Thus, we examined the possibility of a tetrameric structure by using FEFF simulations. Three compounds were selected among Ru complexes with different core structures, [(tacn)Ru^{IV}(μ-$O)_3$$Ru^{IV}$(tacn)]-$(PF_6)_2$ (tacn = 1,4,7-trimethyl-1,4,7-triazacyclononane),[15b] [$(py)_2(O)_2Ru^{VI}$(μ-$O)_2$$Ru^{VI}(O)_2(py)_2$] (py = pyridine),[15a] and [$(bpy)_2Ru^{II}$(μ-$C_2H_5O)_2$$Ru^{II}(bpy)_2$]$(PF_6)_2$,[15c,d] whose structures are shown in Chart 1 as 1−3, respectively. FEFF calculations were carried out using their crystal structures. Parts 1−3 of

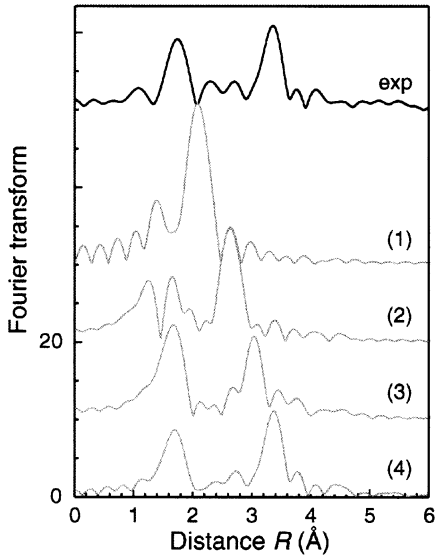

Figure 8. Experimental and simulated EXAFS Fourier transforms for the highly oxidized state of [3,3] (exp) and Ru_2(μ-$O)_2$ complexes. Labels 1−4 are corresponding to those in Chart 1a.

Figure 8 show the simulated EXAFS Fourier transforms for the corresponding Ru_2(μ-$O)_2$ complexes. Figure 8(4) represents the simulation result assuming a structure similar to that of [3,4] with modified Ru−O_w and Ru−(μ-O) distances of 1.79 and 1.85 Å, respectively (vide supra). The Ru_2(μ-$O)_2$ complexes have intense peaks of Ru−Ru scattering between 2 and 3 Å according to the bridging structures. If such a bridge structure were in the highly oxidized state, the corresponding peak should have appeared in this region, as does in some M_2(μ-$O)_2$ examples.[17] Comparison with the experimental Fourier transform clearly excludes the possibility of a tetrameric structure with a diamond core.

End-on peroxide bridging is also one of the possible structures, which might be followed by elimination of O_2. There are few Ru_2(μ-O_2) complexes,[18] and their precise structures are unknown. Thus, centrosymmetric *trans*-[(O)-$(bpy)_2$RuORu$(bpy)_2$(μ-O_2)$(bpy)_2$RuORu$(bpy)_2$(O)] (Chart 1b) was assumed in the calculations, on the basis of the X-ray structure of [3,4] with some corrections of the Ru−(μ-O_2), Ru═O, and O−O distances to 1.95, 1.72, and 1.46 Å, respectively, the last being the average value in some peroxide-bridged Fe[19a] and Co[19b,c] dinuclear complexes. The results of simulation are shown in Figure 9, in which the Ru−O−O angle in the peroxide bridge was varied stepwise by 10° between 180 and 110°. The linear peroxide-bridging gives a Ru−O−O−Ru peak at 5 Å. It becomes weaker and

(16) Wilkinson, E. C.; Dong, Y.; Zang, Y.; Fujii, H.; Fraczkiewicz, R.; Fraczkiewicz, G.; Czernuszewicz, R. S.; Que, L., Jr. *J. Am. Chem. Soc.* **1998**, *120*, 955.

(17) (a) Dong, Y.; Fujii, H.; Hendrich, M. P.; Leising, R. A.; Pan, G.; Randall, C. R.; Wilkinson, E. C.; Zang, Y.; Que, L., Jr.; Fox, B. G.; Kauffmann, K.; Münck, E. *J. Am. Chem. Soc.* **1995**, *117*, 2778. (b) Cinco, R. M.; Rompel, A.; Visser, H.; Aromí, G.; Christou, G.; Sauer, K.; Klein, M. P.; Yachandra, V. K. *Inorg. Chem.* **1999**, *38*, 5988.

(18) (a) Taqui Khan, M. M.; Hussain, A.; Ramachandraiah, G.; Moiz, M. A. *Inorg. Chem.* **1986**, *25*, 3023. (b) Paeng, I. R.; Nakamoto, K. *J. Am. Chem. Soc.* **1990**, *112*, 3289.

(19) (a) Kitajima, N.; Tamura, N.; Amagai, H.; Fukui, H.; Moro-oka, Y.; Mizutani, Y.; Kitagawa, T.; Mathur, R.; Heerwegh, K.; Reed, C. A.; Randall, C. R.; Que, L., Jr.; Tatsumi, K. *J. Am. Chem. Soc.* **1994**, *116*, 9071. (b) Timmons, J. H.; Niswander, R. H.; Clearfield, A.; Martell, A. E. *Inorg. Chem.* **1979**, *18*, 2977. (c) Ramprasad, D.; Gilicinski, A. G.; Markley, T. J.; Pez, G. P. *Inorg. Chem.* **1994**, *33*, 2841.

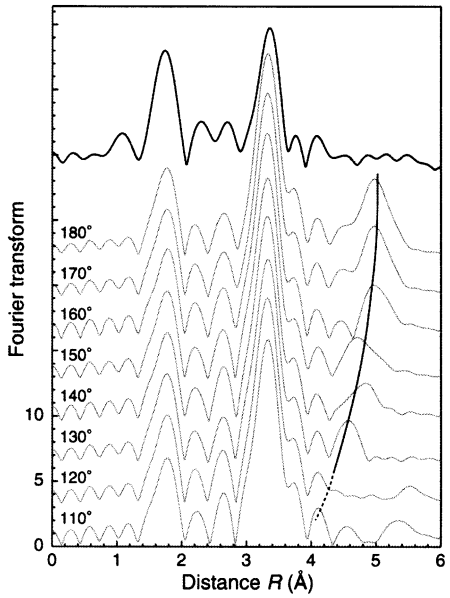

Figure 9. Experimental and simulated EXAFS Fourier transforms for the highly oxidized state of [3,3] and centrosymmetric *trans*-[(O)(bpy)$_2$RuORu(bpy)$_2$(μ-O$_2$)(bpy)$_2$RuORu(bpy)$_2$(O)] (Chart 1b) complexes with various Ru−O−O angles, respectively.

shorter at smaller Ru−O−O angle due to the focusing effect and disappears at 120° with appearance of the next Ru−Ru peak around 5.5 Å. Although determination of the scattering intensity by FEFF calculation is difficult, these comparisons exclude further dimerization of the Ru−O−Ru dimers in the highly oxidized precipitate. It is also supported by the fact that its experimental EXAFS Fourier transform resembles that of the [3,4] state and it is well simulated using the fitting result (Figures 2 and 3). It should be noted that the Ru−O−O(peroxide) scattering hardly affects the EXAFS spectra. The Ru−O−O distance is ∼3.4 Å at the linear conformation, which is between the Ru−N−C(bpy) double scattering path and the strong Ru−(μ-O)−Ru scattering path. The interference among these paths causes only small *decrease* of the peak intensity at 2−3 Å in the Fourier transform, as revealed by the FEFF simulation.

Yamada et al. found that the resonance Raman spectra of frozen solutions with a large excess of Ce^{4+} have features solely different from that of [5,5] and attributed this behavior to Ce^{4+} bonding to the oxo ligands.[4j] Although this was also considered in the FEFF calculation, strong and complex interference between Ru−O−Ce and Ru−O−Ru scattering with similar path lengths made the results ambiguous. However, the proposed six-membered ring structure requires large structural rearrangement with the O−Ru−Ru−O torsional angle ∼0° with the typical O−Ce length of 2.3 Å in cerium tetrakis(β-diketonate) complexes.[20] Though the possibility of such ion association cannot be eliminated, the similarity of the EXAFS spectra along the reaction process does not suggest large structural changes.

(20) Andersen, W. C.; Noll, B. C.; Sellers, S. P.; Whildin, L. L.; Sievers, R. E. *Inorg. Chim. Acta* **2002**, *336*, 105.

Water Oxidation Mechanism. EXAFS results showed that the dimer structure remains roughly unchanged even in the oxidation states higher than the [3,4] state. The direct intramolecular O−O bond formation between two O_w ligands requires a bent Ru−O−Ru structure, and the intermolecular O−O bond formation would have a tetrameric structure as an intermediate, but neither of them was observed. Hurst et al. proposed a Ru−O−OH bond formation between O_w and solvent water.[4e,j] In this mechanism the water association can be stabilized by the bridging oxygen atom, though the bond would not be detected by EXAFS spectroscopy.

What was detected in this study is not a short-lived intermediate itself but the metastable state. However, if the former requires a large structural rearrangement, the latter should have a structure that allows the rearrangement to follow. The unchanged dimer structure obviously excludes the intramolecular O−O formation, since the O_w ligands are very far from each other in the proceeding state. The tetrameric structure would also be unlikely, at least with a more linear peroxide bridge than the focusing limit of photoelectron multiple scattering, ∼140°.

Conclusions

Structural changes upon oxidation of an oxygen-evolving complex, [Ru(bpy)$_2$(H$_2$O)]$_2$(μ-O)O^{4+}, were studied by means of XAFS spectroscopy. The XANES spectra showed that the six-coordinated structure is kept with slight enhancement of a preedge shoulder indicating some symmetry lowering. The EXAFS spectra were also similar among the three oxidation states, and the Ru−O−Ru scattering peak intensity indicated that the highly oxidized samples have an almost linear Ru−O−Ru bridge as in the lower oxidation states. The interatomic distances and the bridging angles were evaluated by the EXAFS curve-fitting analysis, revealing the existence of a short Ru═O bond and the linear bridge structure. The possibility of the "dimer-of-dimers" structure indicated by Raman spectroscopy was ruled out using the FEFF simulations. These results will contribute to clarifying the details of the water oxidation reaction by providing structural information on the high oxidation states.

Acknowledgment. We are grateful to experimental support by Prof. Masaharu Nomura, Dr. Noriko Usami, and Mr. Atsushi Koyama (KEK-PF) and Drs. Tomoya Uruga and Hajime Tanida (JASRI/SPring-8). This work was performed under the approval of the Photon Factory Program Advisory Committee (Grant 2001G142) and JASRI's Proposal Review Committee (Grant 2002B0150-NX-np). This study was supported by a Grant-in-aid for The 21st Century COE Program for Frontiers in Fundamental Chemistry from the Ministry of Education, Culture, Sports, Science, and Technology. K.O. also acknowledges the financial support of the Japan Society for Promotion of Science Research Fellowships for Young Scientists.

IC034373N